University of Saskatchewan
Subatomic Physics Internal Report
SPIR 139

Preliminary Design Considerations for HeTIC

Ward Andrew Wurtz

7th April 2008

Contents

1 Introduction

The Experimental Nuclear Physics Group at the University of Saskatchewan desires to make precision measurements of the $^4\mathrm{He}(\gamma,n)$ cross section using the Blowfish Neutron Detector Array. The photon source employed in this work is the High Intensity Gamma Source (HIGS) at Duke University in Durham, NC, USA. In this document we will describe a proposed target for performing such a measurement, called the Helium Target Ionisation Chamber (HeTIC).

The goal of the proposed experiment using HeTIC is to make very accurate measurements of the $^4\mathrm{He}(\gamma,n)$ cross section at a few, well-chosen energies. We desire to find the differential cross section as a function of polar and azimuthal angles.

We need to make a decision between a gas and liquid target. The liquid target has the advantage of a much higher density, but the disadvantage that it would not be active and requires a cryogenic system to maintain liquid helium. The gas target can be made active. However its density is much lower and therefore the number of neutrons emitted is much less. In having a gas target we can discriminate between background events and require a coincidence between the target and the neutron detectors. This will allow us to lower our detector thresholds and examine low-light output neutron events that can not be discriminated from gamma-ray events by pulse shape discrimination (PSD). By lowering the detector threshold we greatly increase the efficiency of the detectors and therefore increase our count rate. If we made the gas target long and segmented we can greatly increase its effective thickness, which increases the count rate. Since the HIGS photon beam is high flux, we will be able to generate enough photons to make the experiment worthwhile with a target with low effective thickness. Another reason for choosing a gas target is the lower cost of implementation as no cryogenic system is needed.

To estimate a neutron count rate we take a HIGS beam with total flux 10^8 photons/s, of which 10% are viable after collimation giving us a usable flux of $\Phi = 10^7$ photons/s [Wu]. Assume that the cross section is on the order of 1 mb, our target is at atmospheric pressure (101.3 kPa) and room temperature (300 K) and that one segment of our target is $t = 8.0$ cm long (the choice of 8.0 cm will be discussed in section 3). Using the ideal gas law and Bolzman's constant, $k_B = 1.380 \times 10^{-23}$ J/K, we find that the number density of our gas is

$$N = \frac{P}{k_B T} = \frac{101.3\ \mathrm{kPa}}{1.380 \times 10^{-23}\ \mathrm{J/K}\ \times 300\ \mathrm{K}} = 2.4 \times 10^{25}\ \mathrm{atoms/m^3} = 41\ \mathrm{mol/m^3} \tag{1}$$

using Avogadro's number, $6.022 \times 10^{23}\ \mathrm{mol}^{-1}$. Using the atomic mass of helium, 4.00 g/mol, we find that the density of our target is 0.16 mg/cm^3 giving an effective thickness of 1.3 mg/cm^2. Using our estimate of the cross section we can compute the number of interactions,

$$N_I = \Phi\sigma N t = (10^7\ \mathrm{s}^{-1})(1\ \mathrm{mb})(2.4 \times 10^{25}\ \mathrm{m}^{-3})(0.08\ \mathrm{m}) = 2.0\ \mathrm{int/s} = 7000\ \mathrm{int/h}. \tag{2}$$

With one neutron produced per interaction and Blowfish covering $\frac{1}{4}$ of the 4π sterradian spherical shell, we expect about 1800 neutrons to pass through a detector. Assuming an efficiency of 20% we therefore detect around 350 neutrons every hour. With 88 detectors, this makes only 4.0 neutrons per hour on each detector. To obtain 10,000 total events, or 110 per detector, we need 28 hours of beam time. Processing four energies would take 112 hours.

While this may seem very slow, we must remember two things. First, the flux reported by Wu is only an estimate and we have taken the worse case situation. It is our hope that the flux will be much higher by the time this experiment is to occur. Second, we are discussing only one 8.0 cm segment.

HeTIC is designed to use nine useful segments and two end segments. This will increase the data rate 10 fold but it must be noted that each segment will have a slightly different angular coverage due to its position in the array.

2 Kinematics

2.1 Conservation of Energy and Momentum

We can use conservation of nonrelativistic energy and momentum to compute a relationship between the angles that the particles are emitted and their energies. We use the coordinate system as shown in figure 1. The incoming photon brings energy E_γ and breaks apart the nucleus with reaction threshold

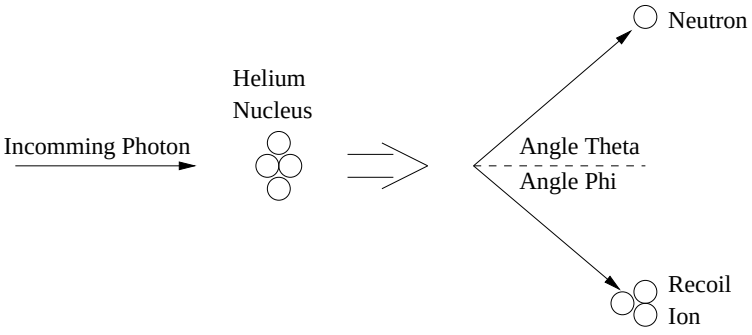

Figure 1: The reaction $^4\mathrm{He}(\gamma,n)^3\mathrm{He}$

E_{th}. The neutron and ^{3}He recoil nucleus are emitted with energy and momentum E_n, p_n, E_3 and p_3. From momentum and energy conservation we obtain three equations

$$E_\gamma - E_{th} = E_n + E_3 \tag{3}$$

$$p_n \sin\theta = p_3 \sin\phi \tag{4}$$

$$\frac{E_\gamma}{c} = p_n \cos\theta + p_3 \cos\phi \tag{5}$$

and from nonrelativistic kinematics we can relate the energy and momentum of the massive particles by

$$E_n = \frac{p_n^2}{2m} \tag{6}$$

$$E_3 = \frac{p_3^2}{6m} \tag{7}$$

where c is the speed of light and m is the mass of a proton or neutron. If we know the energy of the incoming photon, E_γ, then we have six unknowns and five equations. Therefore, if we measure the angle that the neutron is emitted, θ, then we can completely determine the energy of the two resulting particles and the initial direction of the ^{3}He ion. Solving these equations for p_n gives

$$p_n = \frac{1}{4}\frac{E_\gamma}{c}\left[\cos\theta \pm \sqrt{\cos^2\theta - 4 + \frac{24mc^2(E_\gamma - E_{th})}{E_\gamma^2}}\right]. \tag{8}$$

It is a simple matter to substitute this into equation 6 to find E_n. However, it is not a neat solution and equation 8 is very useful in numerical computations. It should also be noted that the '$-$' solution causes $p_n < 0$ due to $mc^2 >> E_\gamma$ as the $24mc^2(E_\gamma - E_{th})/E_\gamma^2$ term dominates under the square root. This contradicts our positive assumption on p_n in figure 1 and we use only the '$+$' solution. The kinetic energies of the reaction products for a 24 MeV photon beam are shown in figure 2. The maximum

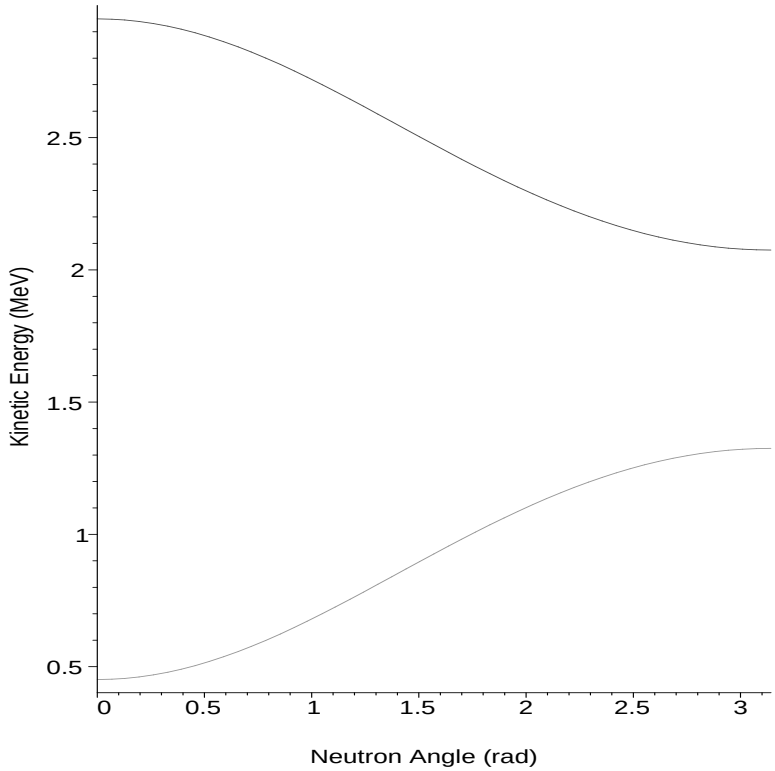

Figure 2: The kinetic energy of the neutron (top) and ^{3}He ion (bottom) emitted from a $^4\mathrm{He}(\gamma,n)^3\mathrm{He}$ reaction with E_γ = 24 MeV

energy of the ^{3}He ion occurs when the neutron is backscattered, or equivalently when $\theta = 180^\circ$. This is useful as it will give us an idea of the range of the ^{3}He ion in the gas. The minimum energy of the ^{3}He ion occurs when the neutron is emitted in the forward direction $\theta = 0^\circ$.

2.2 Stopping Power and Range

The neutron has the ability to leave the target and interact with one of the detectors in Blowfish. However, the charged ^{3}He ion will not be able to escape due to its electric charge. The question we must now consider is how far, after obtaining kinetic energy through the $^4\mathrm{He}(\gamma,n)^3\mathrm{He}$ reaction, does the ^{3}He ion move.

Data using ^{3}He ions is scarce, but we can extrapolate on a result of Santry and Werner to aid us. These authors found that "stopping values for ^{3}He ions are identical to ^{4}He ions at the same velocity" [SW]. Notice that the stopping powers are the same for the two ions at the same velocity, not energy. Using the nonrelativistic equation for energy we find that the stopping power of a ^{3}He ion with energy E_3 is the same as the stopping power of a ^{4}He ion with energy $E_4 = \frac{4}{3}E_3$. In other words, the stopping power is the same for the ^{3}He and ^{4}He ions with the same energy per unit atomic

mass. The work of Santry and Werner is done on carbon, aluminum, silicon, nickel, silver and gold. In order to apply their result we must extrapolate it to helium. Since range is computed directly from stopping power with corrections for multiple scattering [Leo], the results of Santry and Werner apply to the particle's range as well.

The continuous-slowing-down approximation (CSDA) range of an alpha particle moving through helium is available from the National Institute of Science and Technology (NIST) through the ASTAR database [BCZC] and is shown in figure 3. The range is given in units of g/cm^2 and this can be

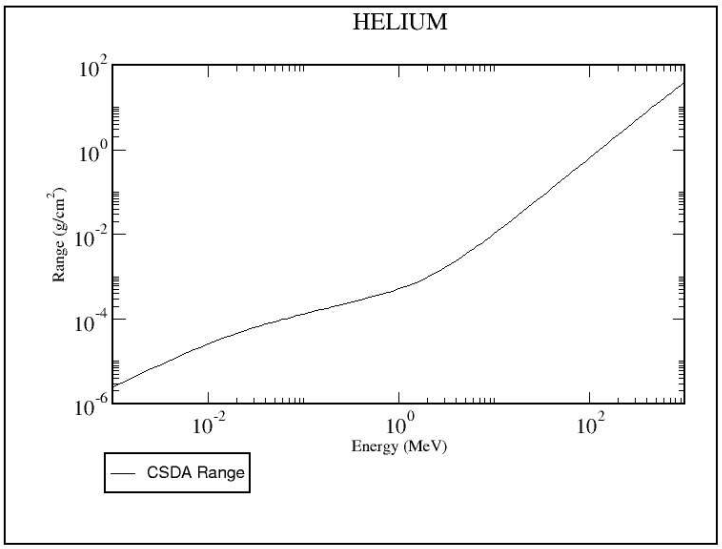

Figure 3: The range of an alpha particle in helium from [BCZC]

transformed into range in units of length by dividing the density. Using figure 3 and the results of Santry and Werner, we can estimate the range of ^{3}He ions in our target.

Let us do an example range calculation. A ^{3}He ion emitted in a $^4\mathrm{He}(\gamma,n)^3\mathrm{He}$ reaction initiated by a 24 MeV photon will have maximum energy 1.3 MeV, as can be seen from figure 2. It will have a range equal to an alpha particle with energy 1.7 MeV. From figure 3 we see that this alpha particle has a range of 2.9×10^{-4} g/cm^2. At atmospheric pressure and room temperature our target has a density of 0.16 mg/cm^2 giving a range of 1.8 cm. In this case the ^{3}He ion may come to rest within our detector. However, as photon energies increase, the range increases and the ions will hit the cathode, anode or walls of the chamber.

2.3 Ionisation

A recoil ^{3}He ion will loose its energy to the helium gas by transferring energy to helium atoms in its path. Some of this energy will create ion/electron pairs and the number of such pairs is quite predictable. The W-Value tells us how much energy is required to create a single pair and Fano factor is an empirical factor that gives the variance in the number of pairs by multiplying it against the variance expected from Poisson statistics [Knoll]. For alpha-particles in helium, the W-value and Fano factor have been measured to be (43.3 ± 0.3) eV/pair and 0.24 ± 0.02 respectively [IKD]. Since the W-value and Fano factors only slightly vary with particle type [Knoll] we can use these values for our ^{3}He ions.

It should be noted that in an ionisation chamber, the noise is dominated by the electronics, not the statistics of ion/electron pair creation [Knoll].

Once the electrons and ions have been liberated, they will drift apart if an electron field is applied. In our target we are concerned only with the electrons as they move much faster than the ions. The drift velocity of an electron through a gas is proportional to the electric field but inversely proportional to the pressure. Figure 4 shows the electron drift velocities for ^{4}He as measured by Bowe [Bowe] and Nielsen [Nielsen]. Note that the drift velocity is a function of electric field over pressure, E/P, since

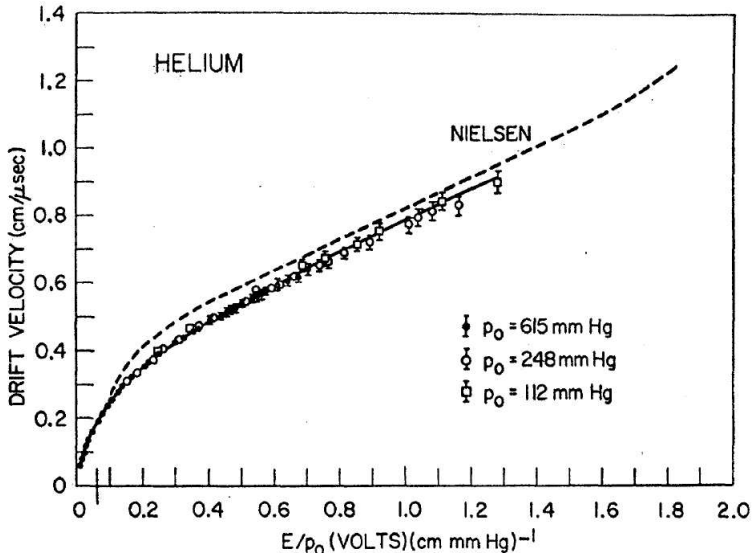

Figure 4: The electron drift velocity of Bowe (points, solid line) and Nielsen (dashed line) from figure 4 of [Bowe]

the datapoints taken at different pressures align. Notice also that, except for a region at low E/P, the drift velocity is essentially linear with E/P.

3 The Active Target Design

Having chosen to construct a gas target, we must consider the principle under which the active target will operate. Noting that noble gases are often used to construct ionisation detectors [Knoll, Leo] we will consider implementing a helium-based ionisation detector. Ionisation detectors operate in one of three modes depending on the geometry and applied voltage: ionisation chamber, proportional counter and Geiger-Mueller counter. The Geiger-Mueller counter and proportional counter are sensitive to low-energy events, making them less suited for our application than the ionisation chamber. Because no gas amplification occurs in the ionisation chamber, it is not sensitive to events that deposit only a small amount of energy, such as a Compton scattering event. This will be examined in greater detail with the simulation in section 5. A recoiling ^{3}He ion, on the other hand, can deposit a few MeV worth of energy and can be detected with an ionisation chamber.

The geometry of an ionisation chamber is generally very simple: a parallel plate capacitor. Neglecting edge effects, the electric field inside such a device is very simple, uniform and has magnitude $E = V/d$ where V is the voltage applied to the plates and d is the distance between plates. The geome-

try we will consider is two plates inside a helium gas container with the photon beam running through them.

The size of and distance between the plates will be determined by the overall length of the detector, the number of segments desired, the size of the photon beam, the space required around the photon beam and the detector response. For this design we will chose 11 segments. The upper limit on the number of segments is set by the available electronics. Eleven is a good number as all the segments can be serviced with a 12 channel ADC. With more segments we are able to achieve a greater position resolution inside the detector. An odd number of segments is desired so that there is a single segment at the centre of the array.

We can chose a length for our segments by taking the radius of Blowfish, 40.6 cm [Swatzky]. If we fit 11 segments into the 81.2 cm diameter, the segments are 7.4 cm long and if we use 9 segments the segments are 9.0 cm long. We desire a compromise with the first and last segment being used mainly for improving our knowledge of the target length and aiding the second and second-last segments. If we chose the segments to be 8.0 cm long, then the inner 9 segments are 72 cm long and the entire active target is 88 cm long. This will give us a target that makes uses of the entire volume of the array and by using the segments nearer the ends, we can achieve measurements at polar angles near 0° and 180°.

Each segment will need a positive anode and negative cathode. The cathodes will all be connected to ground and we can use a single plate of aluminium to construct them. The anodes will be separate and each one will have a separate amplification system. We need 11 aluminum plates separated by a small amount to make the anodes. A conceptual diagram of this system is shown in figure 5.

We must now find the width of the segments and the distance between the plates. The width of the segments is limited on the small side by the diameter of the photon beam, 3.8 cm, and on the large side by our desire to construct a target that will fit inside the array. We need the segment to be wide enough so that every ^{3}He recoil nucleus is able to deposit a sufficiently large quantity of energy in the gas before leaving the parallel plate capacitor. We use the Geant4 simulation discussed in section 5 to chose this quantity. A segment width of 8.0 cm appears to be a good compromise.

The distance between the plates is similarly bounded on the small side by the diameter of the photon beam. However, it is restricted by the electron drift velocity through the electric field. If the electric field is too low, the electrons will not drift toward the anode. If we use a plate separation of 6.0 cm and a voltage of 1000 V, as is the maximum of many preamplifiers, then we achieve an electric field of 17,000 V/m. With a pressure of 1 atm this gives an E/P of 17,000 V/(m atm) or 0.22 V/(cm mmHg) as 760 mmHg is atmospheric pressure. Looking at figure 4 we see that this is the minimum electric field required before the drift velocity falls off non-linearly. We should be able to achieve an electron drift velocity of 0.4 cm/μs. At this drift velocity it would take an electron 15 μs to travel from the cathode to the anode. Note that any attempt to create a pressurised target will drop the drift velocity into the nonlinear region of figure 4 and will require other design changes.

Having selected the width of each section and the separation distance between the anode and cathode we can now draw the cross section of the target, which is done in figure 6. This diagram uses a chamber body of inner diameter 15 cm.

Now that we have found the geometry of a section we can compute its capacitance. The capacitance is computed from the formula for the capacitance of a parallel plate capacitor. Given a length $\ell = 8.0$ cm, width $w = 8.0$ cm, separation distance $d = 6.0$ cm and using the permittivity of free space $\varepsilon_0 = 8.85 \times 10^{-12}$ F/m as an approximation, we can find the capacitance,

$$C = \frac{\ell w \varepsilon_0}{d} = 0.94 \text{ pF} \tag{9}$$

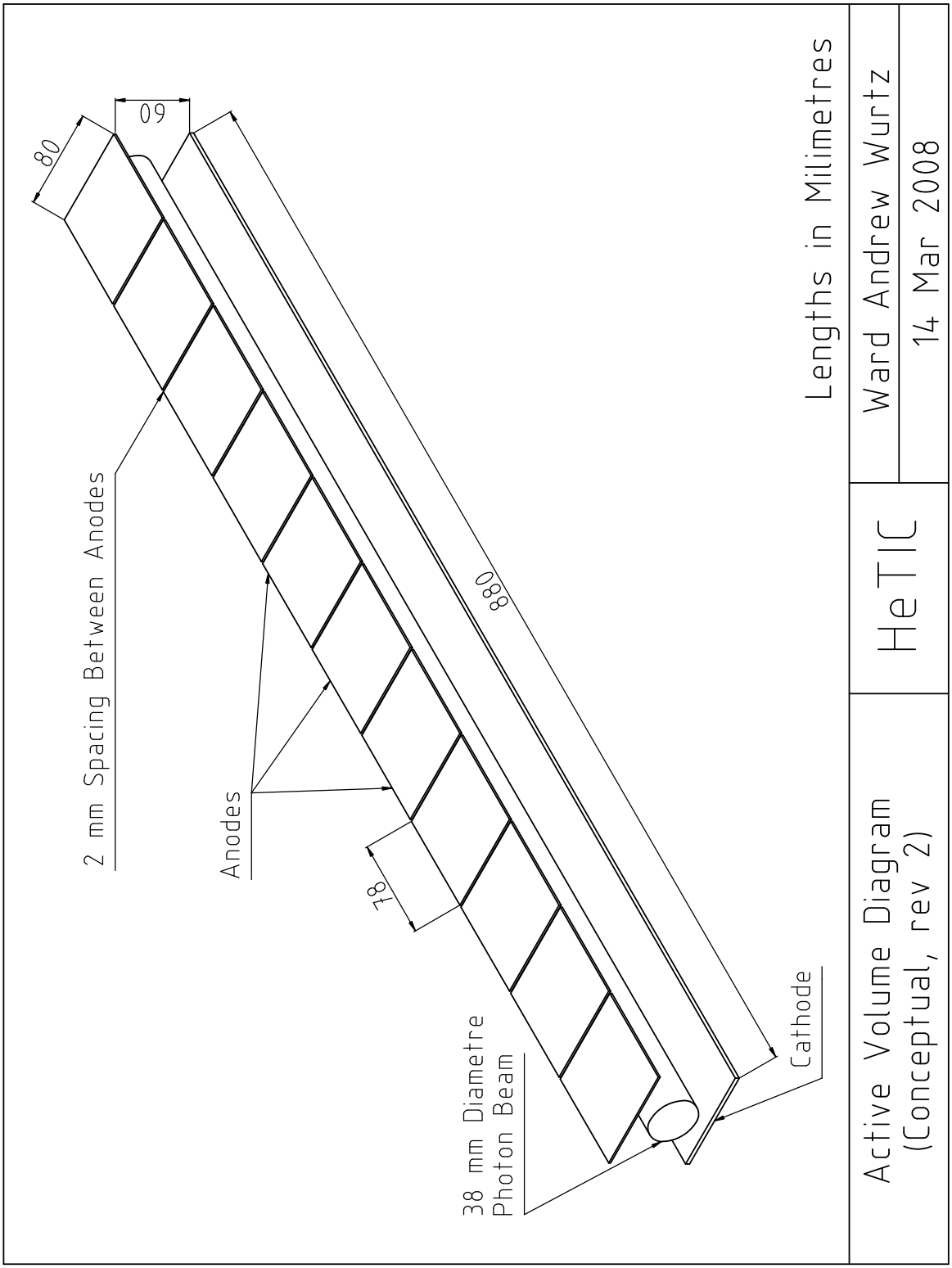

Figure 5: HeTIC active volume conceptual diagram

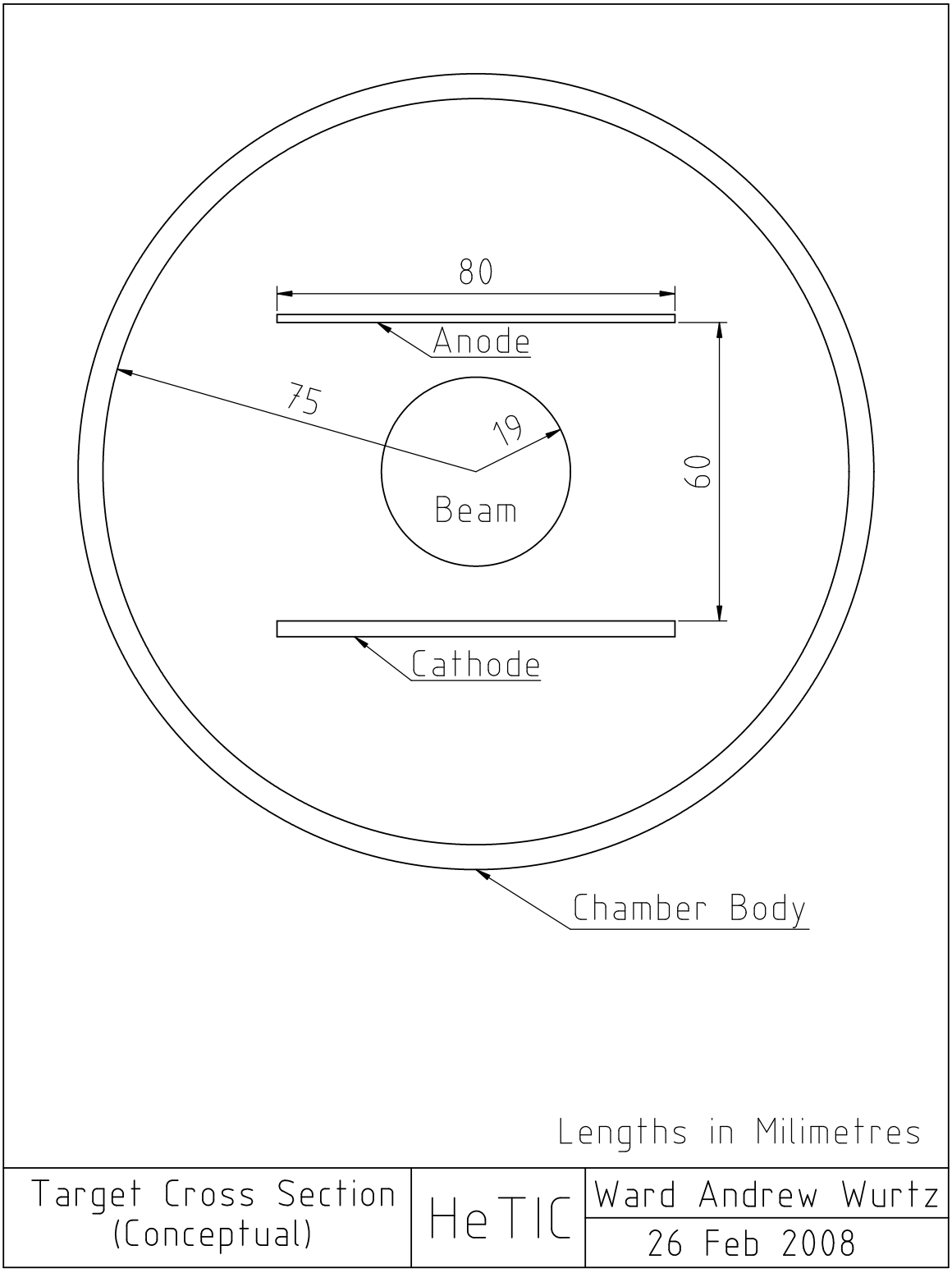

Figure 6: HeTIC cross section conceptual diagram

which is very small. The capacitance will be dominated by the capacitance of any coaxial cables linking the segment to its preamplifier, which may have a capacitance on the order of 100 pF/m [Leo]. We should also note that we have not explicitly accounted for the capacitance of the anode and the chamber body, which should also be dominated by the capacitance of the cable.

A good derivation of the response of this device is given on pages 149 to 152 of [Knoll] and the following discussion is taken from this derivation. Ignoring the positive ions which move too slowly for our needs, the time response is linear and given by

$$V_R = \frac{Q}{Cd} v_d t \tag{10}$$

where $Q = ne$ is the absolute value of the charge deposited in our detector, d is the separation distance, C is the capacitance, v_d is the drift velocity of the electrons and t is the time since the interaction. Note that the response will increase linearly until the electrons reach the anode. It will achieve its maximum value at

$$V_{max} = \frac{Q}{C}\frac{x}{d} \tag{11}$$

where x is the distance travelled by the electrons. We immediately notice that the response is proportional to the distance between the interaction point and the anode. Therefore, two identical events at different positions in the detector will have different responses. This will make it impossible to discriminate between the $^4\mathrm{He}(\gamma,n)^3\mathrm{He}$ and $^4\mathrm{He}(\gamma,n)p\mathrm{D}$ reactions based on the target response. It is possible to use a Frisch grid to produce a response that does not depend on the reaction position [Knoll]. However, this will make timing more difficult as it may take up to 15 μs for electrons to reach the anode and, with a Frisch grid, no response will be recorded in this time. The Frisch grid is also not practical as the range of a ^{3}He ion, as discussed in section 2.2, is larger than the segments and therefore the recoiling ion will not deposit all of its energy inside of the active volume.

We note that if we require a 1 m length of cable, giving a capacitance of 100 pF, a ^{3}He ion depositing 1.0 MeV of energy giving 2.3×10^4 ion pairs (W-value 43.3 eV/ion pair), we obtain a response of

$$V_{max} = \frac{Q}{2C} = \frac{(2.3\times10^4)(1.6\times10^{-19}\mathrm{C})}{2\times100\mathrm{pF}} = 18\ \mu\mathrm{V} \tag{12}$$

if we use interaction distance $x = d/2$. However, if we were able to build our own preamplifier directly at the segment, then the capacitance would be on the order of 1 pF and the response would be 1.8 mV.

4 The Chamber Body

We require a structure to contain the helium gas and active target volume. This structure must also be able to mount inside Blowfish. Since the active target volume is very long, the chamber body must also be very long.

The proposed design for the chamber body is to use a long tube made out of steel or aluminum. Aluminum is preferable from a physics standpoint as neutrons interact with it less than steel while steel is easier to weld. A test of the two materials showed only a small difference for neutorn scattering. We used the simulation described in section 5 to fire 100,000 neutrons at a detector in a pencil beam from the centre of the target. With the threshold used there were 48,658 ($\sigma = 221$) hits on the detector when using the aluminum body and 47,223 ($\sigma = 217$) when using the steel body. There is about a 3%

difference in the number of neutrons detected, which is small but significant. This difference should be correctable by the simulation, which will be needed to correct for scattering no matter which material is used.

In order to seal the ends of the tube, we will need to attach some form of end caps. This will likely require the welding of a flange to the end so that the end caps can be connected with bolts. Such a design can be seen in figure 7.

Regardless of the material used, we must chose some rough dimensions for the chamber body. In figure 7 we used an inner diameter of 15 cm and a length of 240 cm. The inner diameter is chosen roughly and can be adjusted based on the availability of materials. It was chosen to fit through the 21.6 cm hub of Blowfish. Note that it is very important that any flange also be able to fit through the hub to allow mounting of the target. The length is chosen so that the target protrudes beyond the ends of the hubs. This allows for a mount to be built to attach the target to the frame of Blowfish.

The thickness of the chamber body must be chosen based on material availability. From considering neutrons passing though it, thinner is better. The material must be strong enough to be self supporting. Also, up until now we have only considered using atmospheric pressure. However, we must consider pressure buildup that is either intentional or accidental. We want the body to handle high pressures so that if there is a failure, it occurs at the ends of the target and the neutron detectors are not damaged.

The hoop stress (stress around the curve) on a cylinder in the thin shell approximation is given by

$$\sigma_{hoop} = \frac{PR}{t} = 2\sigma_{long} \tag{13}$$

where R is the cylinder radius, t is the material thickness, P is the internal pressure and σ_{long} is the longitudinal stress (stress along the length of the cylinder) [Chattopadhyay]. Note that since the hoop stress is larger than the longitudinal stress we can consider only the hoop stress. To estimate the needed thickness we will consider the case when the pressure unintentionally increases to five atmospheres, 506.6 kPa. We will use a radius of 7.5 cm (diameter of 15 cm) and the yield strength of aluminum, 95 MPa [BJ]. This gives a thickness of

$$t = \frac{PR}{\sigma_{hoop}} = \frac{(506.6\text{ kPa})(7.5\text{ cm})}{95\text{ MPa}} = 0.04\text{ cm} \tag{14}$$

which is very small. Any reasonable thickness of material will be acceptable based on pressure considerations. The target chamber can be easily designed so that it will not fail in the chamber body cylinder due to an unintentional increase in pressure and this will protect the delicate neutron detectors.

Since the chamber body of HeTIC is quite large, we must consider its weight as it must be liftable. The cross sectional area of a tube with inner radius 7.5 cm and thickness 0.64 cm (1/4 inch) is

$$A = \pi(R_{inner}^2 - R_{outer}^2) = \pi((8.1\text{ cm})^2 - (7.5\text{ cm})^2) = 29\text{ cm}^2 \tag{15}$$

which gives a volume of $V = Ah = (29\text{ cm}^2)(240\text{ cm}) = 7000\text{ cm}^3$. The density of steel is 7.9 g/cm^3 [BJ] so we can compute the mass of the chamber body as 55 kg (121 lbs). This is quite heavy, but not unmanageable. It is another reason for making sure the chamber body walls are as thin as possible and for using aluminum, which as a density of only 2.7 g/cm^3 [BJ].

Now that we have a conceptual design for the target body, we can consider how to build the end caps. We have the added concern that photons must pass though the end cap and we wish to impede these photons as little as possible. The Compton scattering cross section is directly proportional to

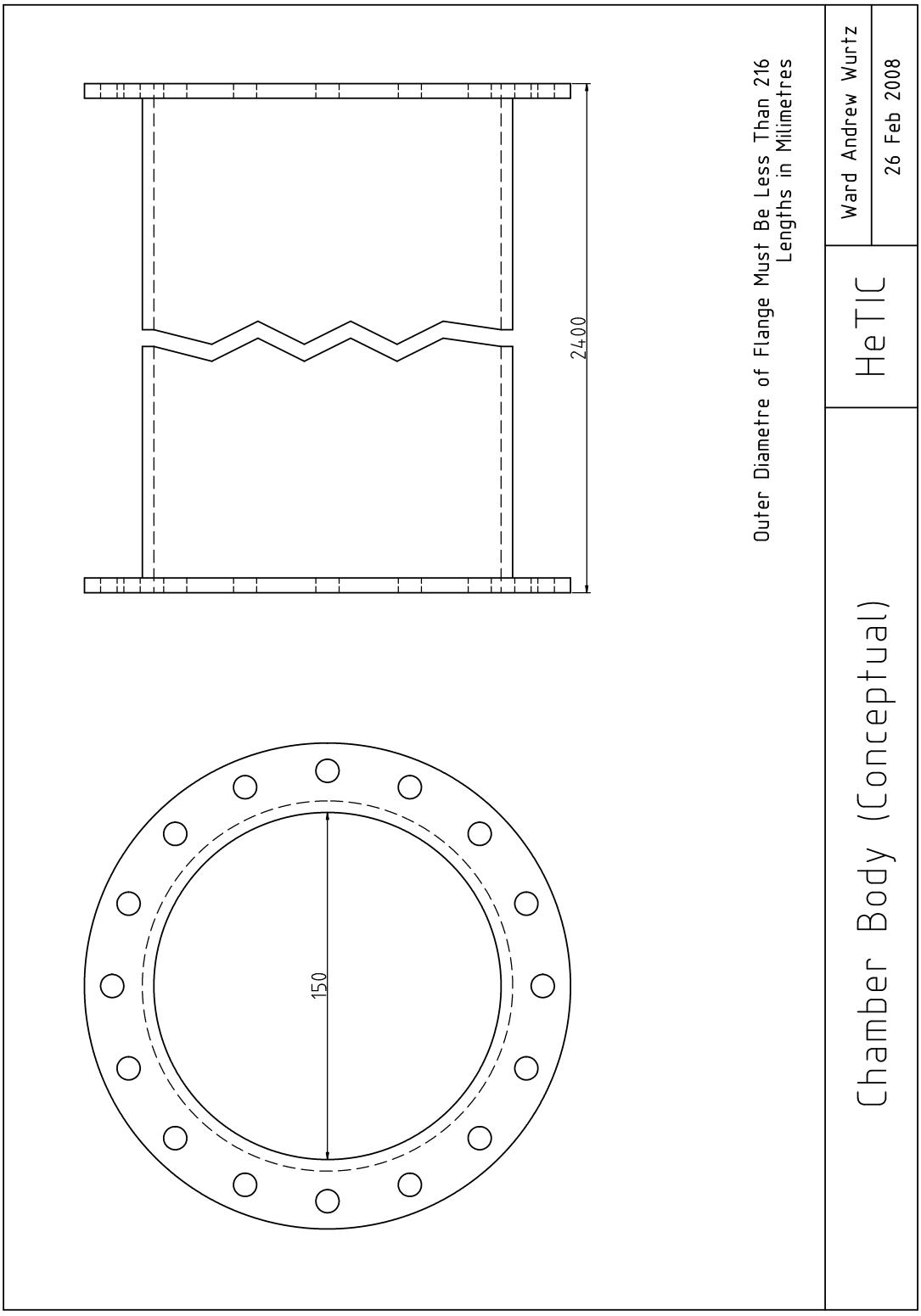

Figure 7: HeTIC chamber body conceptual diagram

the atomic number [Knoll] and we therefore wish to use a material with low atomic number, such as aluminium.

It would be highly desirable to use a dome-shaped end cap as this kind of end cap could take massive amounts of pressure. However, this would be very difficult to create in the dimensions that we require. We must instead use another geometry. It is possible to construct an end cap out of a flat sheet of aluminum, and such a design is shown in figure 8. This end cap has an outer radius meant to match the flange on the chamber body of figure 7.

For a circular plate that is clamped around the edges the maximum radial stress is given by

$$(S_r)_{max} = \frac{3PR^2}{4t^2} \tag{16}$$

which occurs at the edge and top surface. The maximum tangential stress is given by

$$(S_\theta)_{max} = \frac{3(1+\nu)}{8}\frac{PR^2}{t^2} \tag{17}$$

occurring at the centre and top surface of the plate [Chattopadhyay]. Poisson's ratio, ν, appears in equation 17 and is defined as the absolute value of the lateral strain over the axial strain [BJ]. Poisson's ratio is on the order of $\nu = 0.3$ [Chattopadhyay].

Since $(S_r)_{max} > (S_\theta)_{max}$ we can use equation 16 to make a rough estimation of the thickness required. Using a radius of 10 cm and the same pressure and yield strength as before, 506.6 kPa and 95 MPa respectively, we find the thickness required is

$$t = \sqrt{\frac{3PR^2}{4(S_r)_{max}}} = \sqrt{\frac{3(506.6\text{ kPa})(10\text{ cm})^2}{4(95\text{ MPa})}} = 0.63\text{ cm}. \tag{18}$$

Note that 0.64 cm (1/4 inch) thick sheets of aluminum are inexpensive, readily available and easy to machine. Also note that we have made several assumptions in our calculations that are not going to transfer to the real world. We have not taken into account holes made in the end cap for bolts or coaxial cable connections. We cannot assume that the end caps can survive five atmospheres of pressure. The above calculation is for illustration only. It is interesting that the weakest link in the target chamber is on the ends. Therefore, if a failure does occur, it will occur here and be directed away from Blowfish.

While we certainly need a reasonably thick sheet of aluminum to build the end cap, we can modify it to allow the beam to pass through with fewer interactions. We can reduce the plate thickness at the centre of the end cap, as is done in figure 8. If we use a 3.8 cm diameter HIGS beam, we need only make the reduced thickness area slightly larger, say a diameter of 4.5 cm. We can once again use equation 16 to estimate the required thickness

$$t = \sqrt{\frac{3PR^2}{4(S_r)_{max}}} = \sqrt{\frac{3(506.6\text{ kPa})(2.3\text{ cm})^2}{4(95\text{ MPa})}} = 0.15\text{ cm}. \tag{19}$$

We can greatly reduce the thickness at the beam spot.

We must take into consideration the bolts that connect the end cap to the chamber body. The force on the endcap from 5 atm of pressure is given by

$$F = \pi R^2 P = \pi(10\text{ cm})^2(506.6\text{ kPa}) = 16\text{ kN}. \tag{20}$$

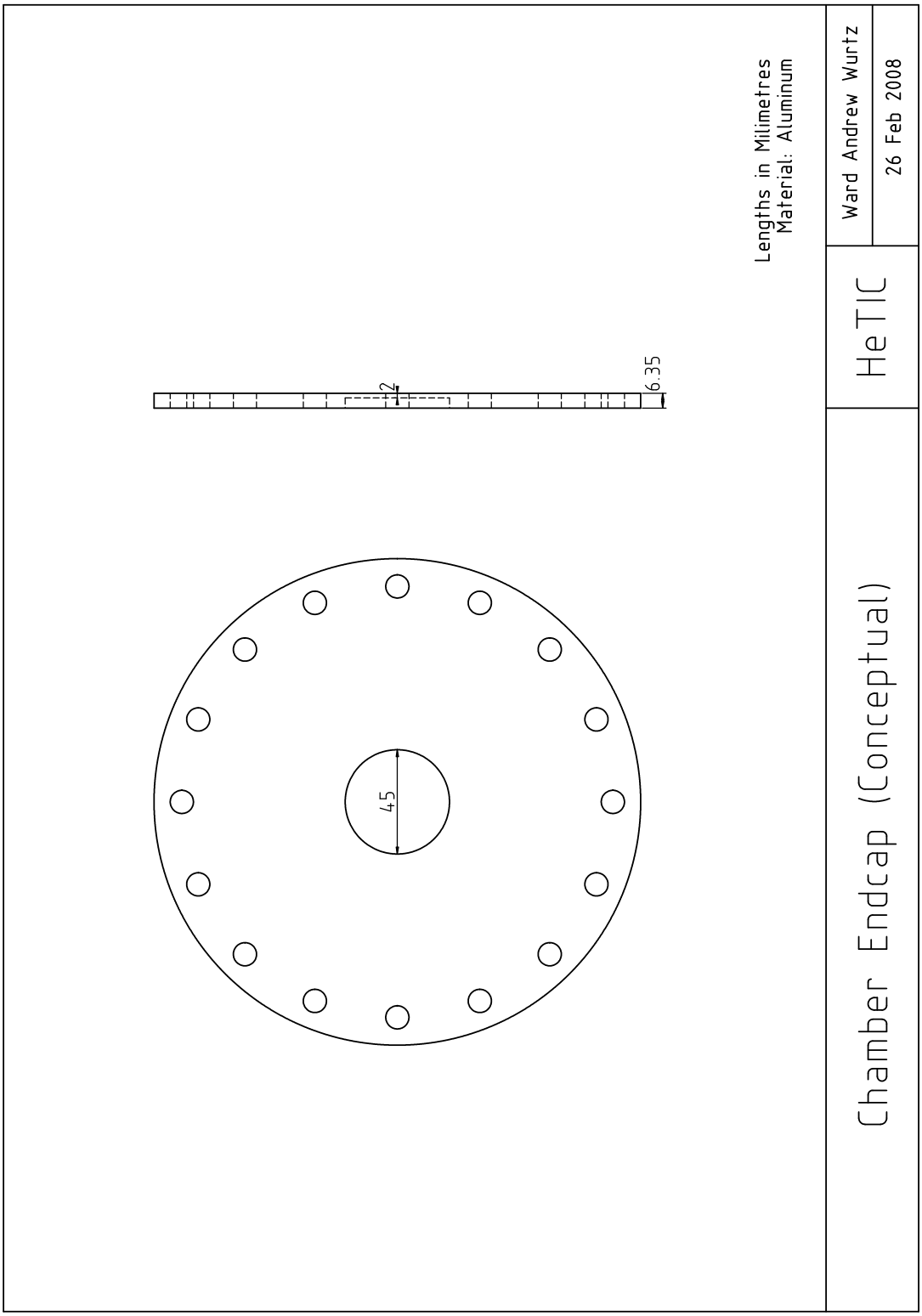

Figure 8: HeTIC end cap conceptual diagram

In figures 7 and 8 we use 16 bolts so the force per bolt will be 1.0 kN. If we use the yield strength of steel, 260 MPa [BJ], we can compute the needed radius of the bolt

$$R = \sqrt{\frac{F}{\pi P}} = \sqrt{\frac{1.0\text{ kN}}{\pi(260\text{ MPa})}} = 1.1\text{ mm}. \tag{21}$$

Since this is very small, any reasonable steel bolt should work.

Once again, it is important to note that the calculations done here are only designed to sketch what may be reasonable for a pressure vessel. Any attempt to actually construct a pressure vessel will require a much more detailed analysis and empirical tests. If the target is to be maintained at atmospheric pressure only, then the above illustrates that the target will be able to handle additional pressure in the case of an unintentional increase in pressure. If the target chamber is to fail, it will fail at the ends which should prevent damage to Blowfish and the neutron detectors.

5 The Simulation

The Geant4 Simulation Toolkit [Geant03, Geant06] can be used to simulate Blowfish and HeTIC. The simulation shown in figure 9 is built from the BlowfishX Simulation Template. It incorporates the

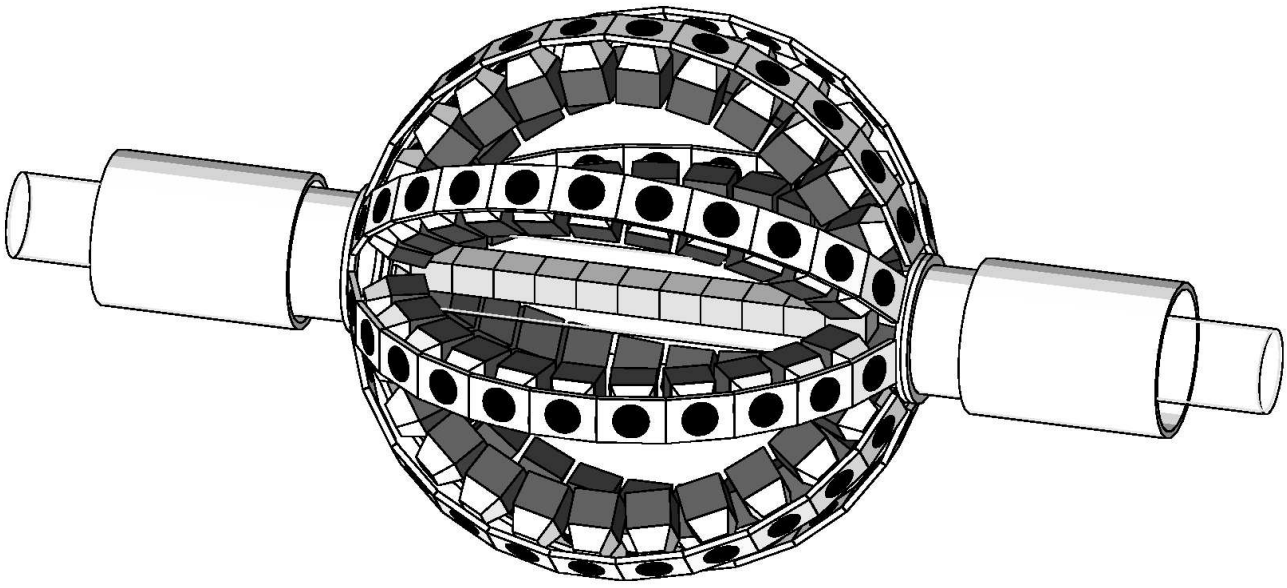

Figure 9: The Geant4 simulation of Blowfish and HeTIC

detectors and aluminum arms of the array. The hubs have also been included, mainly to help visualise what the target will look like in the actual array. The chamber body has been made a wire frame in this figure in order to show the inside of the target. Notice the eleven active target segments and how they are distributed in the array. Also notice how the ends of the chamber body extend beyond the hubs.

Each segment of HeTIC can be treated as a sensitive detector in Geant4. It is very easy to find the energy deposited in each section as this information is given to us by Geant4. However, it is more difficult to find the response, given in equation 11. We need to also extract the position of the event,

which we compute as the average position of the particle during the sensitive detector hit. By using the W-value we are able to convert the energy deposited by the particle into electron/ion pairs and find the charge of the travelling electrons. Using this information, we are able to compute V_{max}.

We must note that the actual response of the detector will be greater than what we have estimated. We are assuming that only electrons liberated between the parallel plates will have an effect. However, since the chamber body must be grounded, electrons outside of the plates will also have an effect, increasing the response. The electric field in this region is not simple as it is between the parallel plates so we cannot quantify this effect without using more sophisticated numerical techniques. The response generated by the simulation should be interpreted as the minimum response.

It is possible to examine a number of features of our detector by looking at some simple applications of our simulation. For example, we can look at the effects of the electromagnetic processes on signals from HeTIC. We used a pencil beam of 30 MeV photons fired upstream of HeTIC. The simulation used 10^6 photons and examined the energy deposited in the active volume segments. The energy deposited was never more than 35 keV and almost always less than 20 keV.

Let us contrast this against the energy deposited by a ^{3}He ion after a photodisintegration reaction. We can compute the kinetic energy of this ion using the kinematics described in section 2.1. We simulated 10^5 photodisintegration events due to a 30 MeV pencil photon beam. These events occurred at a single location, the centre of the target. The resulting energy deposited in the target and the target response are shown in figure 10. Notice that there is a large separation between the minimum response

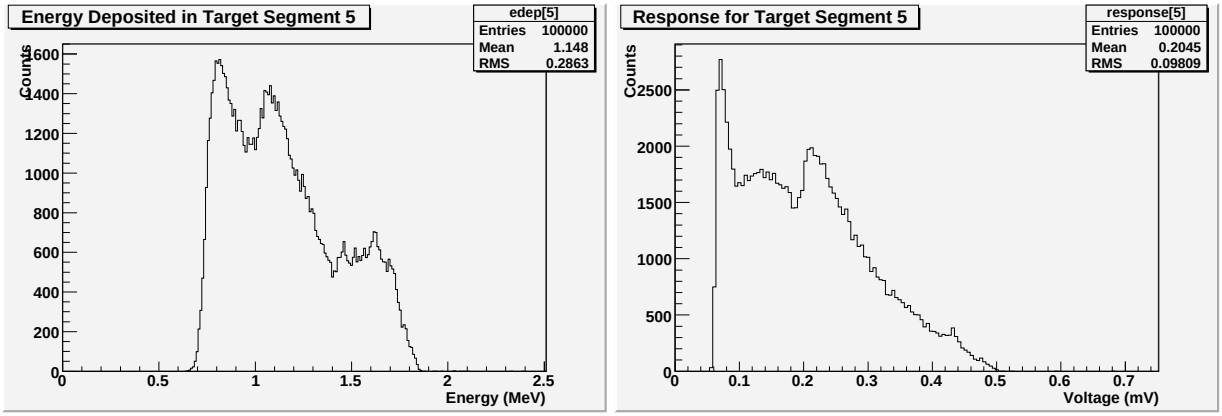

Figure 10: The energy deposited and response histograms for ^{3}He ions produced from photodisintegration reactions caused by 30 MeV photons in the centre of a target segment

and zero. It should be possible to set the threshold low enough that we can detect all photodisintegration events. Also, the downstream segments detected many events as the more energetic ^{3}He ions travelled through many segments. The upstream segments only detected a few events as these ions had less energy, as governed by the calculations of section 2.1.

The previous simulation was overly ideal. It can be easily modified to present a more accurate picture by emitting the ^{3}He ions at a random position distributed as they would be for a uniformly distributed 3.8 cm diameter photon beam. The resulting energy deposited and detector response can be seen in figure 11. Notice that both the energy deposited and response histograms now go to zero. This is due to ions entering the segment after being created in a different segment and coming to a stop quickly. However, an ion that does not deposit enough energy in this segment to be detected will have deposited enough in a different segment.

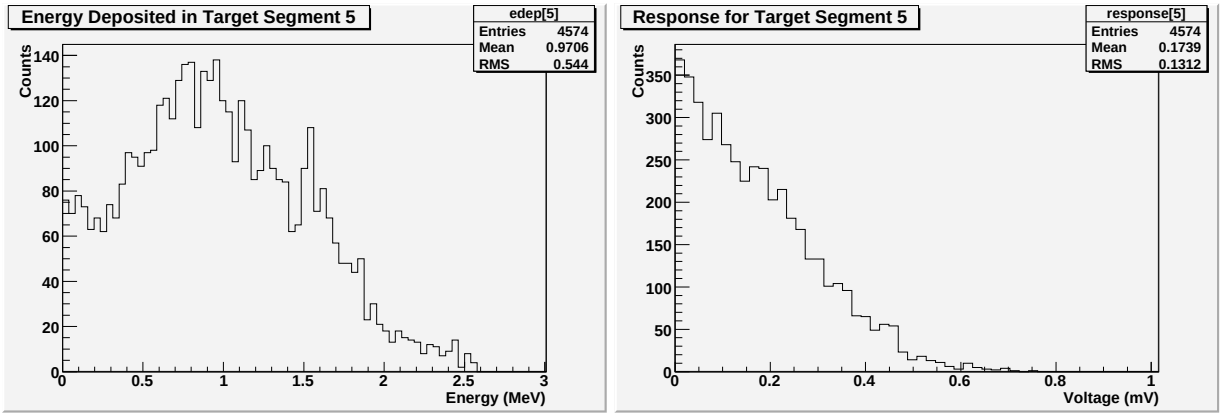

Figure 11: The energy deposited and response histograms for ^{3}He ions produced from photodisintegration reactions caused by 30 MeV photons in a 3.8 cm diameter beam

In this section we have seen that, in principle, it should be possible to use HeTIC to detect photodisintegration reactions while screening electromagnetic reactions. The noise in the system will determine what level the thresholds can be set at and this will determine if HeTIC can operate with 100% efficiency.

6 Available Hardware

The University of Saskatchewan Experimental Nuclear Physics Group has a stockpile of equipment retained from the former Saskatchewan Accelerator Laboratory. In order to construct HeTIC, we will need a preamplifier and amplifier for each section (assuming we don't build our own preamplifier for this project). We will also need a peak sensing ADC, TDC, descriminator, high voltage supply and scaler. Note also that the amplifier may require a 93 Ω coaxial cable to connect it with the preamplifier as opposed to the regular 50 Ω cables. Currently we have available the following electronics modules:

- 18 Ortec 142B preamplifiers (8 are new-in-box)
- 21 Ortec 460 delay line amplifiers
- 6 EG&G CF8000 8 channel constant fraction discriminators
- 2 Le Croy 2259A 12 channel peak sensing ADCs
- 1 CAEN V775 32 channel TDC
- 2 Le Croy HV4032A positive voltage modules with 4 channels each

7 Testing and Implementing the Design

Now that the preliminary design is finished, a proof-of-concept test must be performed before a more detailed design can proceed. This will require building a small test bed. The electronics to do so are all

available at the University of Saskatchewan. However, a working model of the detector will have to be built and this means that money must be made available for this project.

Scott Specialty Gases lists a 24 cm diameter by 152 cm height cylinder of research purity helium gas at about $900 on their website. Therefore, any test system setup must efficiently use the gas so that it is not wasted.

When materials have been selected, a way to mount the anode and cathode plated in the chamber body must be constructed. The electronics must be connected to the active target segments and a gas system must be designed. A mounting system must be designed in order to mount the target inside of Blowfish.

The preliminary design for an active ^{4}He target has been completed. This target will be able to make a high-accuracy measurements of the $^4\mathrm{He}(\gamma, n)$ cross section and determine the angular dependence of this reaction. Much work yet remains on a detailed design and testing before an experiment can be performed using HeTIC.

References

[BCZC] M.J. Berger, J.S. Coursey, M.A. Zucker and J. Chang, *Stopping-Power and Range Tables for Electrons, Protons, and Helium Ions.* National Institute of Standards and Technology, http://physics.nist.gov/PhysRefData/Star/Text/contents.html (Accessed 27 Mar 2007).

[BJ] F. P. Beer and E. R. Johnston, Jr., *Mechanics of Materials, SI Metric Edition.* McGraw-Hill, Toronto (1981).

[Bowe] J. C. Bowe, Phys. Rev. **117**, 1411 (1960).

[Chattopadhyay] S. Chattopadhyay, *Pressure Vessels: Design and Practice.* CRC Press, Boca Raton, Florida (2005).

[Geant03] Geant4 Collaboration, Nucl. Instr. and Meth. A **503**, 250 (2003).

[Geant06] Geant4 Collaboration, IEEE Trans. Nucl. Sci. **53**, 270 (2006).

[IKD] N. Ishida, J. Kikuchi and T. Doke, Jpn. J. Appl. Phys. **31**, 1465 (1992).

[Knoll] G. F. Knoll, *Radiation Detection and Measurement, Third Edition.* John Wiley and Sons, Inc., New York (2000).

[Leo] W.R. Leo, *Techniques for Nuclear and Particle Physics Experiments.* Springer-Verlag, Berlin (1994).

[Nielsen] R. A. Nielsen, Phys. Rev. **50**, 950 (1936).

[SW] D. C. Santry and R. D. Werner, Nucl. Instr. and Meth. **185**, 517 (1981).

[Swatzky] B. D. Sawatzky, *A Measurement of the Neutron Asymmetry in $d(\vec{\gamma}, n)p$ Near Threshold*. PhD Thesis, University of Virginia, Unpublished (2005).

[Wu] Y. K. Wu, *2007 HIGS Performance With 780, 450 and 280 nm FEL Cavity Mirrors*. Unpublished (2007).